Journal of Agricultural Sciences
(Tarim Bilimleri Dergisi)

J Agr Sci-Tarim Bili
e-ISSN: 2148-9297
jas.ankara.edu.tr

JAS

Creation of Gold Nanoparticles with the Use of *Nigella sativa* L. Plant Extract Derived from Agricultural Waste Components and Its Potential as a Biomedical Agent

Mehmet Fırat Baran[a*]

[a]*Batman University, Vocational School of Technical Sciences, Food Technology program, 72000, Batman, TÜRKİYE*

ARTICLE INFO
Research Article
Corresponding Author: Mehmet Fırat Baran, E-mail: mfiratbaran@gmail.com
Received: 24 October 2023 / Revised: 10 February 2024 / Accepted: 11 February 2024 / Online: 23 July 2024

Cite this article
Baran M F (2024). Creation of Gold Nanoparticles with the Use of *Nigella sativa* L. Plant Extract Derived from Agricultural Waste Components and Its Potential as a Biomedical Agent. *Journal of Agricultural Sciences (Tarim Bilimleri Dergisi),* 30(3):570-583. DOI: 10.15832/ankutbd.1380667

ABSTRACT
In this study, gold nanoparticles were rapidly synthesized with a low-cost and environmentally friendly approach through the extract prepared using agricultural waste parts of the *Nigella sativa* L. plant. Properties of gold nanoparticles from *N. sativa* leaf extract UV-visible Spectrophotometer, X-ray diffraction, Electron Disperse X-ray, Zeta potential and Zetasizer, Field Emission Scan Electron Microscopy (FESEM), Atomic Power Microscopy, Transmission Electron Microscopy (TEM), thermogravimetric and differential thermal analysis characterized by its data. It was observed that the morphologies of the synthesized gold nanoparticles (AuNPs) exhibited a spherical appearance with an average size distribution of 107 nm and a monodisperse. In addition, they were found to be stable structures at -17.7 mV surface charge, and maximum absorbance at 538.41 nm. For the usability of AuNPs as biomedical agents, antimicrobial and anticancer effects were evaluated using Microdilution and MTT methods, respectively. It was determined that AuNPs were effective in suppressing the proliferation of 0.02-1.00 µg/mL concentration range on *Staphylococcus aureus* ATCC 29213, *Bacillus subtilis* ATCC 11774, *Escherichia coli* ATCC25922, *Pseudomonas aeruginosa* (ATCC27833) and *Candida albicans* pathogenic strains. The viability of CaCo-2, Skov-3, and U118 cancer cells was effectively inhibited by the produced AuNPs by, respectively, 66.73%, 30.93%, and 23.23%. It has been determined that AuNPs have significant antimicrobial and anticancer effects on hospital pathogens and cancer cell lines.

Keywords: Antimicrobial, Gold nanoparticles, FESEM, MTT, TEM analysis

1. Introduction

The field of nanotechnology is continuously expanding at a rapid pace. Within this domain, there is a growing interest in the study that focuses on the construction of structures that possess superior qualities at the nanoscale. Of particular importance in this sector is the research and development of technologies for the manufacturing of metallic nanoparticles as well as the application areas for these nanoparticles. Metallic nanoparticles contribute a lot to these fields with their superior qualities such as chemical, thermal, optical, magnetic, conductivity, and electronics in nano science and technological fields (Jafarizad et al. 2019; Firdhouse & Lalitha 2020; Punnoose & Mathew 2022). AuNPs, which are nanoscale structures, have many uses in medical applications (Attar & Yapaoz 2018; Donga et al. 2020; Rautray & Rajananthini 2020; Padalia & Chanda 2021) and theranostic applications of various diseases (Parida et al. 2011; Velmurugan et al. 2014; Patra et al. 2015; Kumar et al. 2017; Baran 2019; Mohammadi et al. 2019; Latha et al. 2019; Abu-Dief et al. 2020; Arroyo et al. 2020; Rautray & Rajananthini 2020), in catalysis studies (Zayadi et al. 2019), and in dye removal (Latha et al. 2019).

The manufacture of AuNPs calls for the utilisation of a wide range of methodologies, including biological, chemical, and physical approaches. The use of biological sources in synthesis research has a number of advantages over other approaches, including the ones listed above (Al-ogaidi et al. 2017; Patil et al. 2018; Rolim et al. 2019; Baran & Saydut 2019; Barabadi et al. 2020; Korani et al. 2021). Synthesis studies with plant parts (such as leaves, fruits, and flowers) are among the biologically sourced methods that are simpler, do not pose a threat to human health due to the absence of pathogenicity risk and toxic chemicals, do not require special conditions for welding, obtain more products as a result of synthesis, have a structure that is biocompatible, and bring about low cost advantages. A considerable deal of curiosity is generated by these, not just within the realm of biological approaches but also among other methods (Mythili et al. 2018; Parveen et al. 2019; Nor Azlan et al. 2020; Baran et al. 2021; Chen et al. 2021; Ercan 2023).

In the process of forming AuNPs, the extract that is prepared from plants contains a variety of components that act as reducing agents. These components include flavonoids, vitamins, phenolics, amino acids, polysaccharides, and so on. Following the combination of the extract obtained from plant sources of AuNPs and the metal salt solution, the ionised Au^{+3} valence form in the aqueous structure undergoes bioreduction through the phytochemicals present in the extract, resulting in the transformation of the ionised Au^{+3} valence form into Au^{o} (AuNPs)(Shankar et al. 2016; Some et al. 2019; Donga et al. 2020; Korani et al. 2021).

Ranunculaceae is the family that includes the herbaceous, annual, self-growing, trichome-covered plant known as *N. sativa*. This plant can grow anywhere from 40 to 90 centimetres in height. This herb, which has been around for two thousand years, has made its way from Asia to Europe and Africa. A perennial plant native to Southern Europe and Western Asia, *N. sativa* is a member of the Ranunculaceae family and is grown in many regions of the globe. This medicinal plant, which has been used and considered sacred for thousands of years in traditional medicine systems like Unani, Ayurveda, Siddha, and Tıbb-ā Nebevî, is used not only as a spice in cuisines around the world but also for gastrointestinal disorders, skin diseases, diabetes, cancer diseases, hair loss, and cosmetic purposes. Utilized in skin care products that fight aging and hair loss. In addition to its use as a spice, it has also been employed in the treatment of a variety of ailments, including bronchitis, asthma, hypertension, eczema, and the flu (Davoudi-Kiakalayeh et al. 2017). In terms of its phytochemical composition, it is distinguished by the presence of over one hundred beneficial chemicals, including thymoquinone, thymol, carvacrol, and nigellidine (Ariamanesh et al. 2019).

The purpose of this research was to characterise the properties of AuNPs produced using an extract derived from agricultural waste parts of the *N. sativa* plant cultivated in the Mardin Kızıltepe region, as well as to assess their potential as biomedical agents (antimicrobial and anticancer). The synthesis of AuNPs using an environmentally friendly method was the primary objective of this study.

2. Material and Methods

2.1. N. sativa extract preparation

The plant samples were collected from Mardin (Kızıltepe) in July. Dr. Cumali Keskin from Mardin Artuklu University confirmed the plant samples taxonomic identification. Plant samples were stored in the Herbarium (Voucher No. MAU: 2023-29) of the same institution (İş & Beyatlı 2023). Post-harvest agricultural waste parts of the *N. sativa* plant were washed several times in the Mardin Kızıltepe Station region in June. It was kept on blotting paper in room condition. After drying, 100 g leaf sample was taken and boiled in a 1000 mL glass beaker with 400 mL distilled water. It was then cooled and, filtered. The obtained extract was prepared for synthesis.

2.2. Preparation of hydrogen tetracloroaurate (III) hydrate ($HAuCl_4$) solution

A metal solution with a concentration of 50 millimolar (mM) was prepared to obtain AuNPs by bioreduction from the solid compound of Alfa Aesar, $HAuCl_4$, 99.9% (Kandel, Germany).

2.3. Synthesis of AuNPs

The waste components of the *N. sativa* were utilised in the green synthesis process to produce AuNPs. The straightforward application processes and extremely low cost are two of the benefits of this environmentally safe technology that does not contain any hazardous chemicals. The synthesis of AuNPs in this bottom-up technique is facilitated by redox reactions involving Au^{+3} ions ionised in an aqueous environment; this is possible due to the bioactive components in the plant extract that include amine and hydroxyl groups. Additionally, these components effectively ensure stability and coating. 250 mL of the plant extract and 350 mL of 50 mM $HAuCl_4$ solution were mixed at 200 RPM at 25 °C for five minutes. It was kept without heat treatment, shaking, etc. The maximum absorbance bands of the structure that caused the color change were examined between 300-800 nm by taking samples from the synthesis medium over time, taking into account the intensity of the color change that occurred over time.

2.4. Characterization of AuNPs

To examine the formation of AuNPs with the color change occurring in the synthesis medium and the characteristic maximum absorbance bands associated with it, scans were made for maximum absorbances in the wavelength range of 300-800 nm in the Perkin Elmer One UV-vis device. The crystal structures of the synthesized AuNPs were evaluated using the Rigaku Miniflex 600 model X-Ray Diffraction Diffractometer (XRD) with measurements taken in the range of 20-80 at 2θ. Using the data obtained from these measurements, the calculation was made using the Debye-Scherrer equation to calculate the crystal nano dimensions (Rautray & Rajananthini 2020; Perveen et al. 2021; Uzma et al. 2021). Element contents of the synthesized particles were determined using RadB-DMAX II computer-controlled Electron Disperse X-ray (EDX). In the examination of mass losses of AuNPs against temperature changes, evaluation was made using Shimadzu TGA-50 Thermogravimetric and Differential Thermal Analysis (TGA-DTA) results at 25-900 °C. In the examination of the morphological structures of the synthesized AuNPs, Jeol Jem 1010 Field Emission Scan Electron Microscopy (FE-SEM) and Transmission Electron Microscopy (TEM)

were additionally identified using Park System XE-100 Atomic Power Microscopy (AFM) micrograph images. To determine the stability of AuNPs, Zeta potential, and Zetasizer analysis data were evaluated, respectively, in examining the surface charges and size distributions through a Marven. The functional groups of the phytochemicals responsible for the reduction and stability of the synthesized AuNPs were evaluated by the frequency changes of the spectra read between 4000-650 cm^{-1} by Perkin Elmer One Fourier Transformation Infrared spectroscopy (FTIR).

2.5. Antimicrobial suppressing effects of synthesized AuNPs on hospital pathogens

Nosocomial pathogens of AuNPs synthesized by *N. sativa* plant extract, *Staphylococcus aureus* ATCC 29213 (*S. aureus*), *Bacillus subtilis* ATCC 11774 (*B. subtilis*), *Escherichia coli* (*E. coli*) ATCC25922, *Pseudomonas aeruginosa* (ATCC27833) and *Candida albicans* (*C. albicans*) microorganisms on their growth were determined using the Microdilution method (Baran 2018; Baran et al. 2021a; Baran et al. 2021b). Minimum Inhibition Concentration (MIC) values, which play a role in the antimicrobial effect on these microorganisms, were evaluated with this method. All microorganisms were obtained from Artuklu University Microbiology Research Laboratory, Mardin, Turkey. From the synthesised AuNPs, antibiotics, and $HAuCl_4$, solutions with a concentration of 32 mg/mL were formed. In the first well of each microplate, microdilutions were performed till a final concentration of 2^{10}. To clarify, each dilution phase involved a reduction in concentration of 50% from the prior well, commencing from the initial well. After mixing the media and AuNPs prepared at different concentrations into the microplate wells, microdilution was performed starting from the first well. Some wells were reserved for other control steps of growth. With the same method, in addition, the suppressive effects of antibiotic and $HAuCl_4$ solution on the growth of pathogenic strains were examined for comparison purposes. Vancomycin was used for gram positive *S. aureus* and *B. subtilis* strains, colistin for gram negative *P. aeruginosa* and *E. coli* strains, and additionally flocanozole antibiotics were used for *C. albicans*. After applying the microdilution method, the microplates were incubated at 37 °C for 24 hours. At the end of the period, reproduction control was performed and MIC was defined.

2.6. Anticancer effects of synthesized AuNPs on cancer cell lines that suppress viability

Cytotoxic effects of synthesized AuNPs on cancer cells were investigated by 3-(4,5-dimethylthiazol-2-yl)-2,5-diphenyl tetrazolium bromide assay (MTT) method (Aktepe et al. 2021; Atalar et al. 2021; Baran et al. 2021a; Baran et al. 2021b) in Dicle University Scientific Research Center, Diyarbakır, Turkey. In the application, Colorectal Adenocarcinoma (Caco-2), Glioblastoma (U118), and Human Ovarian sarcoma (Skov-3) lines were used as cancerous cell lines. In addition to these, cytotoxic effects on the Dermal Fibroblast (HDF) healthy cell line were also evaluated. Experimental applications were carried out in 75 t-flasks. Skov-3 cell line was allowed to grow in RPMI medium, other cell lines were allowed to grow in DMEM medium (Dulbecco Modified Eagle), in an oven at 37 °C with 5% CO_2 and 95% air where humidity conditions were provided. Hemocytometer-controlled cell lines were transferred to 96-well microplate wells and left overnight. Then, AuNPs prepared in varying concentrations were added to the wells and the cells were left to interact with the nanoparticles in an oven at 37 °C for 48 hours. After the interaction, MTT and DMSO solutions were waited for 3 and 15 minutes, respectively. Then, the absorbance spectrum of the cells was examined using MultiScan Go Thermo adjusted to a wavelength of 540 nm. By using these absorbances, the concentrations of AuNPs that suppressed the percent viability on the cells and the IC50 (Concentration that constitutes half of the maximum inhibition) values were calculated using the formulas given below (Ahmed et al. 2019; Awad et al. 2019; Baran et al. 2021; Chen et al. 2021; Kumari et al. 2023)

$$\% \text{ Viability} = G/N \times 100 \quad (1)$$

$$IC_{50} = (G-N)/N \times 100 \quad (2)$$

In the equality; G= was used instead of absorbance values of cells after interaction with AuNPs, and N= absorbance values of cells in the absence of AuNPs.

3. Results and Discussion

3.1. Characterization of AuNPs

3.2. UV-vis Data of AuNPs

10 minutes after *N. sativa* extract and $HAuCl_4$ solution were mixed, a color change from yellow to pink-red occurred. With the increase in the intensity of the color change over time, samples were taken from the reaction medium periodically and scans were made for maximum wavelength absorbances using UV-vis (Figure 1). The color change from yellow to pink red occurred due to the formation of AuNPs (Gopinath et al. 2016; Latha et al. 2019; Parveen et al. 2019; Firdhouse & Lalitha 2020). The maximum absorbances obtained in the data were determined at a wavelength of 538.41 nm. These maximum absorbance bands confirmed the formation and existence of Surface Plasma Resonance (SPR) AuNPs, which are formed by the vibrations occurring on the plasma surface due to the formation of AuNPs (González-Ballesteros et al. 2017; Umamaheswari et al. 2018; Latha et al. 2019; Usman et al. 2019; Satpathy et al. 2020a; Chen et al. 2021; Korani et al. 2021; Mandhata et al. 2021).

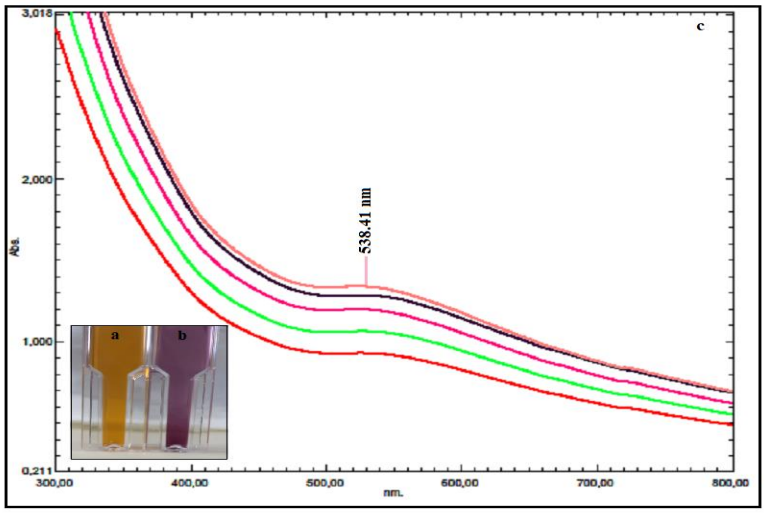

Figure 1- *N. sativa* extract (a), color change due to the formation of synthesized AuNPs (b), and (c) maximum absorbance bands of AuNPs in wavelength scan data

3.3. Crystal pattern and dimensions of synthesized AuNPs via XRD data

Determination of the crystal patterns and nano sizes of the synthesized AuNPs In the analysis performed between 20 and 80 at 2θ using XRD, the presence of Bragg angle expansions taken at the points (111), (200), (220), and (311) in the data, the crystal pattern of AuNPs showed the cubic centered face (fcc) (Figure 2) (Seku et al. 2019; Singh et al. 2019; Küp et al. 2020; Uzma et al. 2021). It has been observed that the structure of the synthesised AuNPs is compatible with the reference card number 05-2870 issued by the Joint Committee on Powder Diffraction Standards (JCPDS). The FWHM values of Bragg angles at points (111), (200), (220), and (311) were found to be 38.45, 44.42, 64.26, and 77.46, respectively. The crystal nanosizes of the synthesized AuNPs were calculated as 20.60 nm using the FWHM value of the high peak (belonging to Bragg's angle) by the Debye-scherrer equation. In the green synthesis studies, it was shown that the crystal nanosizes of AuNPs were calculated as 22.76 nm (Hatipoğlu 2021b) and 27.91 nm (Uzma et al. 2021) through the Debye scherrer equation.

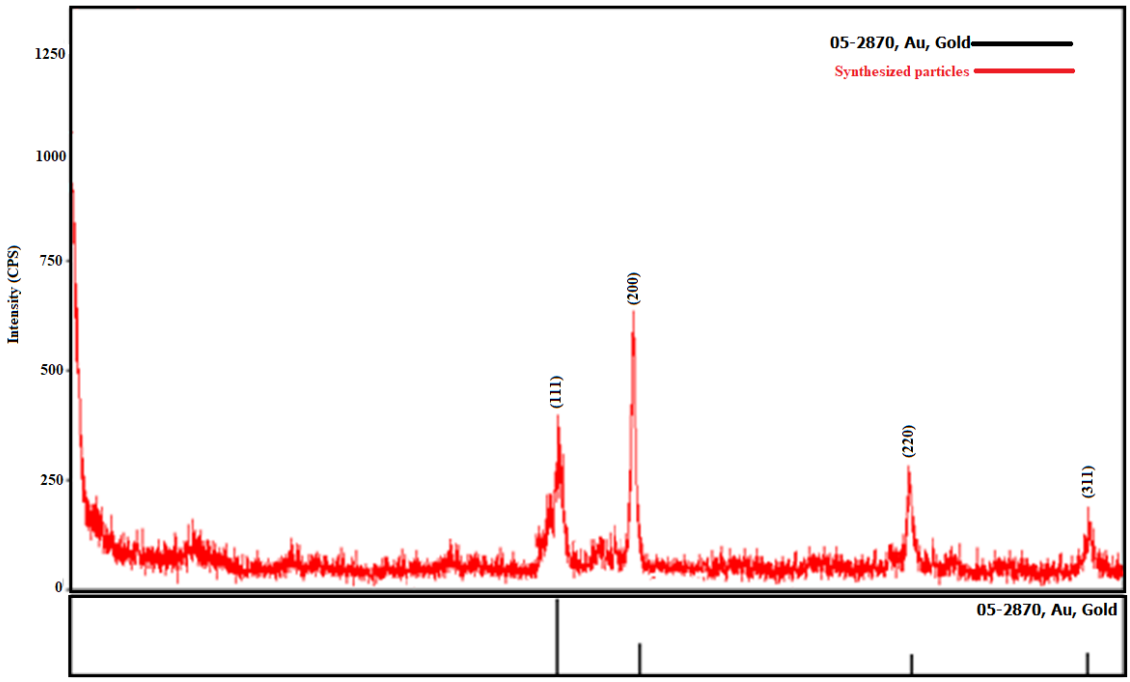

Figure 2- XRD data of the crystal structures of AuNPs synthesized with *N. sativa* extract at 2θ

3.4. Elemental profile of synthesized particles

The EDX profile given in Figure 3 was examined in the analysis of the elemental compositions of the particles synthesized by *N. sativa* extract. The presence of the Au element in the majority of the profile showed that AuNPs were formed. Weak peaks

such as O, and C in the profile were also due to the presence of phytochemicals (Gopinath et al. 2016; Doan et al. 2020; Chen et al. 2021; Hosny et al. 2021; Mandhata et al. 2021; Hosny et al. 2022a).

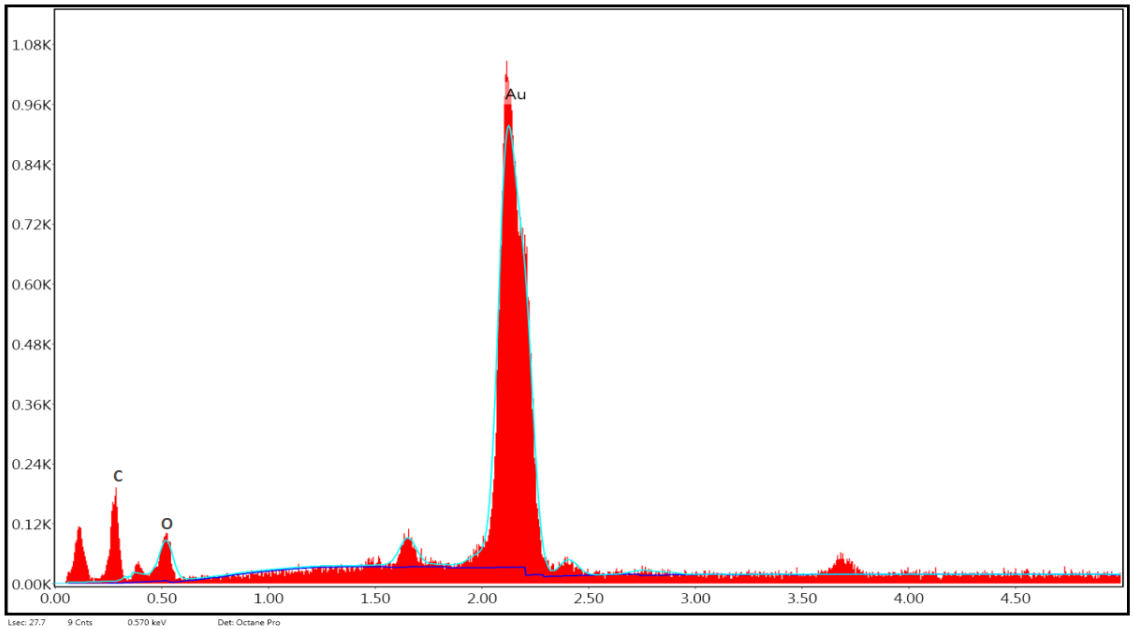

Element	Wt %	Atomic %	Error %	Net Int.	Net Error %	K Ratio	Z	R	A	F
O K	20.49	76.03	14.74	44.16	5.86	0.0476	1.3789	0.7344	0.1685	1.0000
Au L	79.51	23.97	8.82	245.44	7.05	0.8052	0.8823	1.0950	1.0242	1.1207

Figure 3- Elemental compositions of *N. sativa* plant extract green post-synthesis particles

3.5. TGA-DTA analysis of AuNPs obtained using N. sativa extract

The data obtained by performing TGA-DTA between 0 and 1000 °C for mass losses that may occur with the temperature change of the synthesized particles were evaluated. In the graph given in Table 1 and Figure 4, mass losses were observed at four different temperature points. The first mass loss occurred in the range of 27.10-225.29 °C, and the 3.86% mass loss occurred due to the loss of adsorbed water. Mass losses at 226.33 and 800.45 °C were due to the presence of phytochemicals, which are bioorganic compounds (Baran & Saydut 2019; Doan et al. 2020; Sepahvand et al. 2020; Padalia & Chanda 2021). The negative surface charge of -17.7 mV given in Figure 6 also supported the presence of phytochemicals around the synthesized AuNPs. In addition, the presence of peaks belonging to organic compounds in the EDX data given in Figure 5 confirmed this situation.

Table 1- Temperature points where mass losses occur against the resistance of the synthesized AuNPs to heat treatments (n=3, $\bar{X} \pm S\bar{x}$)

Mass Loss Point	*Temperature (°C)*	*Mass Loss (%)*
First	27.10-225.29	3.86±0.28
Second	226.33-350.16	26.59±0.74
Third	351.10-508.90	27.58±0.36
fourth	507.95-800.45	8.20±0.12

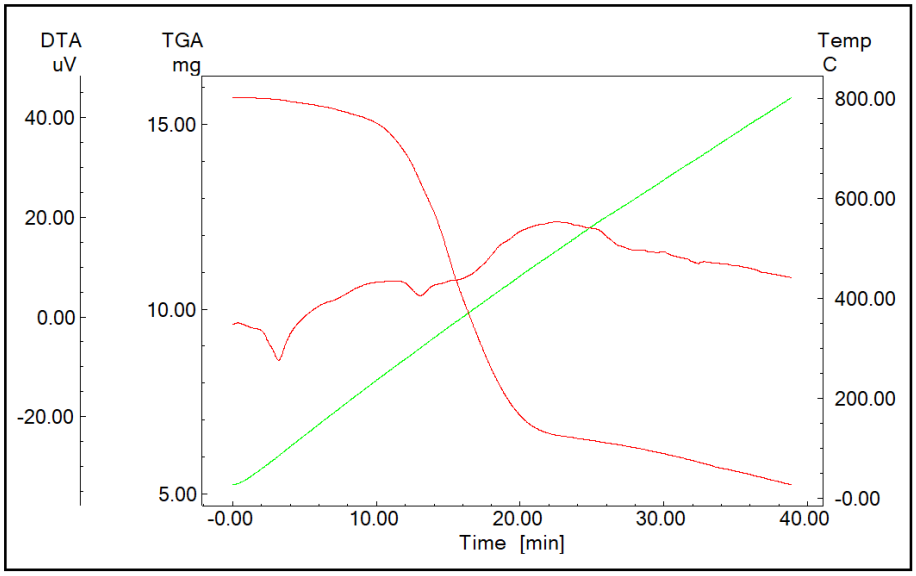

Figure 4- Mass loss points revealed by temperature change in TGA-DTA data of AuNPs obtained as a result of synthesis

3.6. Morphological structures of AuNPs

The morphologies of the synthesized AuNPs were observed spherical in appearance and in a single distribution in the FESEM and TEM images given in Figure 5. AuNPs synthesized with *Annona squamosa* L fruit extract were shown to be spherical and monodisperse in TEM images (Dadigala et al. 2018). In a synthesis study obtained with market plant wastes, it was seen that AuNPs were in spherical morphology (Mythili et al. 2018). In FESEM images of a study with *Elaeis guineensis* leaf extract, AuNPs were spherical in morphology (Ahmad et al. 2018). Similar findings were also found in other environmentally friendly synthesis studies (Ahmad et al. 2018; Usman et al. 2019; Jafarizad et al. 2019; Mousavi-Kouhi et al. 2022). In addition, in the AFM micrograph taken for the morphological structures and topographic distributions of the synthesized AuNPs in Figure 2, it was seen that they had dimensions below about 100 nm, exhibited a monodisperse, and were spherical (Francis et al. 2017; Vinita et al. 2018; Ullah et al. 2019; Rauf et al. 2021).

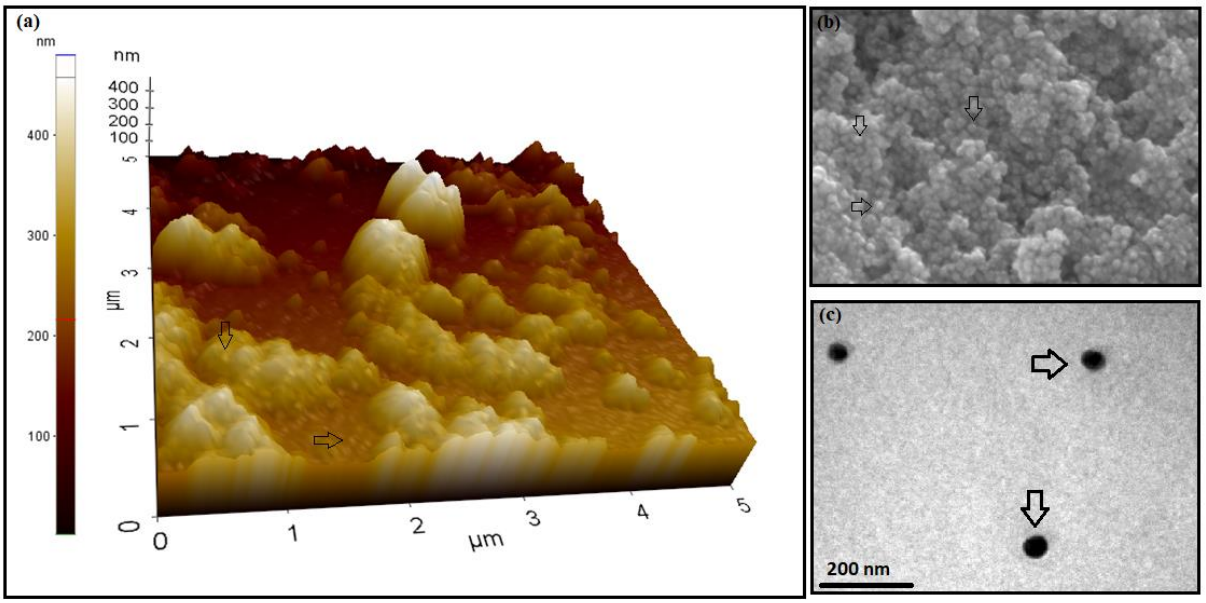

Figure 5- Showing the morphological structures of the synthesized AuNPs; a. AFM, and b. FESEM, and c. TEM micrograph images

3.7. FTIR spectroscopy data

FTIR spectroscopy analysis data were analyzed to examine the functional groups of phytochemicals responsible for bioreduction. In the spectroscopy data given in Figure 6, frequency shifts were observed at 3 different points, 3335.46-3319.70 cm^{-1}, 2124.05-2115.41cm^{-1}, and 1635.63-1634.95 cm^{-1}. These shifts, respectively, belong to alcohol or phenol groups (O–H), alkyne groups (–

C=C–), and amine groups (–NO), and their reduction of Au^{+3} valent metal in aqueous medium to Au^{o}, that is, AuNPs. The findings indicated that hydroxyl/phenol groups, amine groups, and alkyne groups are some of the functional groups that may be involved in the creation and stability of gold nanoparticles (AuNPs) (Usman et al. 2019; Donga et al. 2020; Babu et al. 2020; Baran et al. 2021a).

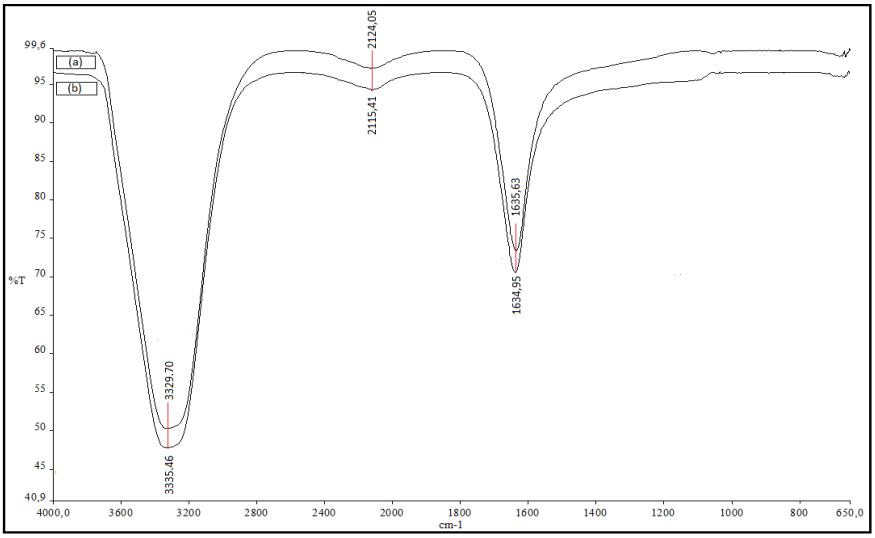

Figure 6- FTIR spectra of functional groups of phytochemicals that are responsible for bioreduction and stability; (a) *N. sativa* and (b) the liquid fraction that was formed as a result of the reaction

3.8. Charge distribution of the surface structures of synthesized AuNPs

The surface charges of AuNPs obtained using *N. sativa* extract are given in Figure 7. The results showed that they had a charge of -17.7 mV. A green synthesis study with *Elaeis guineensis* extract showed AuNPs to be -14.7 mV (Ahmad et al. 2018). In a synthesis study with *Cystoseira baccata* extract, it was shown to be -30.7 mV (González-Ballesteros et al. 2017). In addition, a graph of -19.2 mV surface charges of AuNPs was given in a study conducted with *Cyanthillium cinereum* extract (Punnoose & Mathew 2022).

Phytochemicals (such as alcolloids, and flavonoids) found in plant sources play an important role in stabilization and stability in the negative surface charge formation of AuNPs. The fact that the synthesized particles have only negative surface charges ensures that they are stable and prevents the formation of negative conditions such as aggregation and fluctuation that affect the stability. In addition, AuNPs, which have a negative surface charge, also contribute positively to pH stability, helping them to be effective in challenging circulatory or intracellular physiological conditions. The stable structure of AuNPs also has an important place in medical applications as therapeutic agents (Giljohann et al. 2010; Khan et al. 2019; Webster 2020; Hosny et al. 2022b).

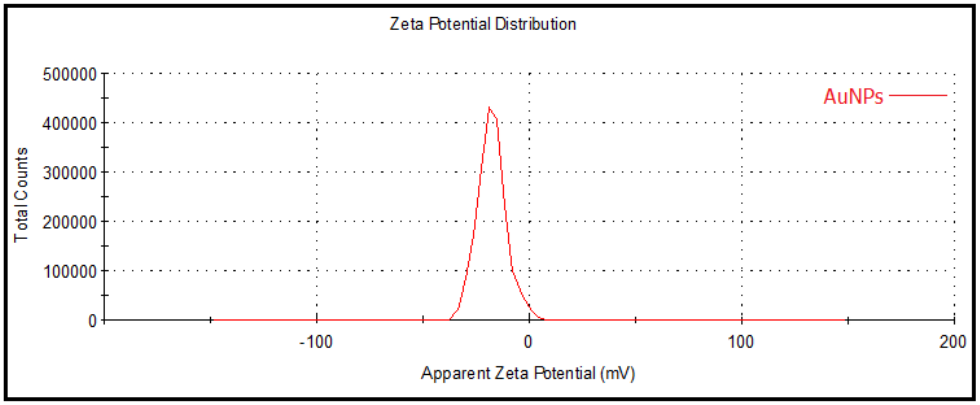

Figure 7- Distribution of surface charges of synthesised AuNPs according to their zeta potential's.

3.9. Density-dependent size distributions of synthesized AuNPs

The hydrodynamic size distributions of the AuNPs that were generated by the extract that was made using waste fractions from *N. sativa* and acquired through DLS are presented in Figure 8. After analysing the data, it was found that the diameters of the

senized AuNPs had a distribution that was, on average, 107 nm. In studies for the synthesis of plant-derived AuNPs, mean zetasize distributions were reported as 96.46 nm (Hatipoğlu 2021b) and 118 nm (Mousavi-Kouhi et al. 2022).

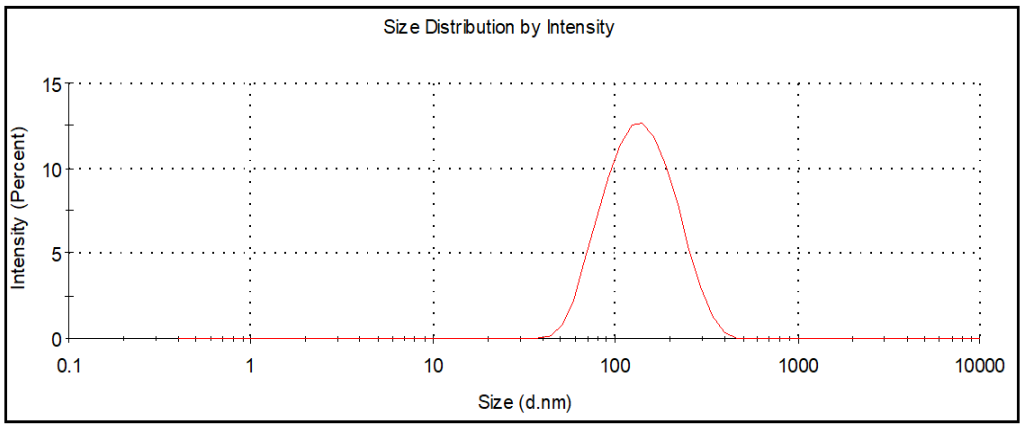

Figure 8- Distribution of density-dependent sizes of synthesized AuNPs

3.10. Antimicrobial suppressing effects of synthesized AuNPs on hospital pathogens

MIC values of AuNPs synthesized using *N. sativa* extract were analyzed by microdilution method in suppressing the growth of hospital pathogen microorganisms. MIC values of 0.02-0.03 µg/mL and 0.50-1.00 µg/mL were determined on the growth of Gram-positive strains and Gram-negatives, respectively. In addition, the MIC value of the synthesized AuNPs on the growth of *C. albicans* was found to be 0.25 µg/mL. AuNPs synthesized in all microorganisms except *P. aeruginosa* showed suppression at very low concentrations from both the antibiotic and $HAuCl_4$ solution. AuNPs, colistin antibiotic, and $HAuCI_4$ solution showed antimicrobial activity at the same concentration on *Paeruginosa* strain (Figure 9 and Table 2).

The AuNPs may exert antimicrobial effects at different concentrations on different strains. Cell wall structure, components, etc. of some strains cause AuNPs to be effective at different concentrations (Donga et al. 2020). In addition to the concentration, properties such as surface charge, shape, and size also play an important role in the antimicrobial effects of AuNPs (Jha et al. 2017). Since microorganisms and NPs are negatively and positively charged in a liquid medium, respectively, NPs interact with electrostatic attraction (Ahmed et al. 2016; Ferreyra Maillard et al. 2018; Babu et al. 2020). Subsequently, adverse changes occur in wall and membrane morphology, such as disruption of membrane potential and permeability. In addition, AuNPs block ATPase functional activity and cause a decrease in ATP level. AuNPs interact with structures where nitrogen, phosphate, sulfur, and oxygen atoms are highly concentrated, such as proteins (Cui et al. 2012; Donga et al. 2020). Another negative effect of NPs is that by increasing the expression of genes involved in redox reactions, they increase the level of Reactive Oxygen Species (ROS) such as -OH, -SO, and -NO. These species bind to important molecules such as proteins, DNA, lipids, and enzymes and adversely affect their structure and functions. All this accelerates biodegradation and causes the death of microorganisms (Cui et al. 2012; Ahmed et al. 2016; Jha et al. 2017; Donga et al. 2020). It was stated that AuNPs obtained in the green synthesis study with *Jatropha integerrima Jacq* extract were effective MICs at 10.00, 5.00, and 2.5 µg/mL concentrations on *S. aureus*, *B. subtilis*, and *E. coli*, respectively (Suriyakala et al. 2022). In a similar study conducted with the *Paecilomyces variotii* bacterial strain, they found that the MIC VALUE was below 0.064 µg/mL. In another synthesis study with *Prunus cerasifera* extract, *S. aureus*, *B. subtilis*, *E. coli*, *P. aeruginosa*, and *C. albicans* 0.25, 0.12, 1.00, 0.50, and 0.50 µg/mL concentrations were reported to be effective in MIC (Hatipoğlu 2021a).

Table 2- MIC values of synthesized AuNPs, antibiotics used for each strain in practice, and $HAuCI_4$ solution have antimicrobial effects on their growth (n=3, $\bar{X} \pm S\bar{x}$, 24 Hours)

TESTED ORGANISM	***AuNPs**** *µg/mL*	***HAuCI₄ Solution*** *µg/mL*	***Antibiotic**** *µg/mL*
S. aureus	0.02±0.001	0.50±0.007	1.00±0.017
B.subtilis	0.03±0.001	0.25±0.002	1.00±0.015
E. coli	0.50±0.018	1.00±0.069	2.00±0.120
P. aeruginosa	1.00±0.067	1.00±0.032	1.00±0.058
C. albicans	0.25±0.004	0.50±0.016	2.00±0.082

:** Solution containing AuNPs synthesized via extract from *N. sativa* waste parts; *:** Solution prepared from $HAuCl_4$ solid compound salt; *****:** Solutions prepared from the antibiotics colistin for gram-negatives, vancomycin for gram-positives, and fluconazole for fungi.
Note: The concentration of each solution used in the preparation was 32 µg/mL.

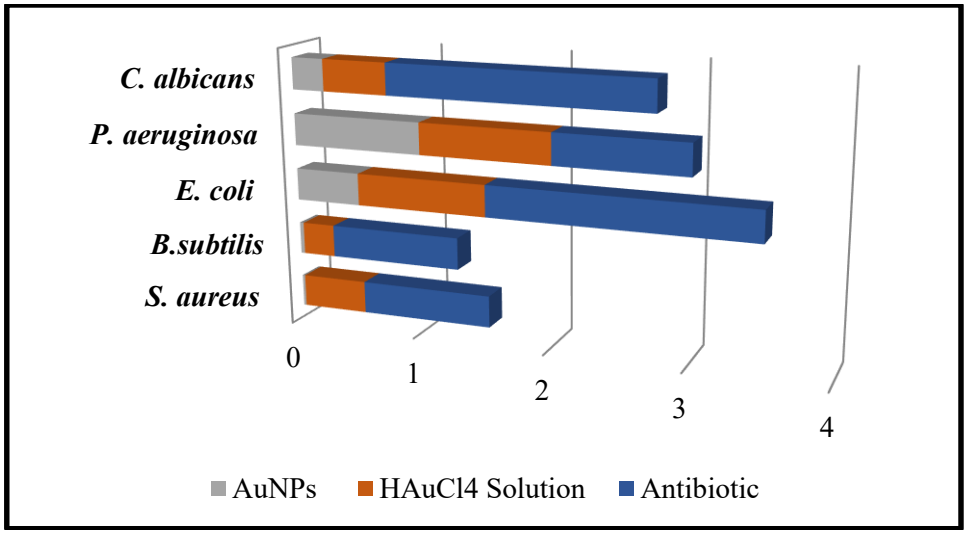

Figure 9- MIC values of AuNPs, $HAuCl_4$ solution, and antibiotics synthesized on the growth of microorganisms. (**AuNPs;** AuNPs synthesized through extract obtained from *N. sativa* waste parts, **$HAuCl_4$ Solution;** Solution prepared from HAuCl4 solid compound salt at 32 µg/mL concentration**, Antibiotic;** Solutions prepared from the antibiotics colistin for gram-negatives, vancomycin for gram-positives, and fluconazole for fungi at a concentration of 32 µg/mL)

3.11. Anticancer effects of synthesized aunps on cancer cell lines that suppress viability

After the interaction of AuNPs synthesized by *N. sativa* extract with cancer cell lines and healthy cell lines for 48 hours, the percent viability of the cells was evaluated. The concentrations of U118, CaCo-2, and Skov-3 cancer cells as well as percent viability suppressing on HDF healthy cell line were determined by the MTT method. As seen in Table 3 and Figure 10, 56.52% viability at 100 µg/mL concentration in the healthy cell line showed that the synthesized AuNPs had no toxic effect. The same concentration caused suppression of 39.93%, 66.73%, and 23.23% in Skov-3, CaCo-2, and U118 cancer cells. It was observed that the concentration of 100 µg/mL was the most effective on the cancer cell CaCo-2 with 66.73% suppression. Even 25 µg/mL concentration produced 30.76% suppression on CaCo-2 cells. The IC_{50} values of AuNPs synthesized on HDF, Skov-3, CaCo-2, and U118 cell lines were calculated as 118.88, 429.92, 174.83, and 632.11, respectively.

Some properties of nanoparticles such as concentration, shape, size, surface charge, interaction time, degree of deposition, etc. play an important role in toxicity (Remya et al. 2015; Swamy et al. 2015; Rolim et al. 2019). AuNPs contact cells through chemical adsorption, electrostatic attraction, hydrophobic interaction, or chemical bonds (Doan et al. 2020; Webster 2020; Mehravani et al. 2021). Tumorous and inflammatory tissues have large vascular vessels and their large pores that allow the passage of substances such as nutrients and oxygen to these areas. It allows nanoparticles to easily collect and pass to these points through these pores (Chen et al. 2021; Hosny et al. 2021). AuNPs that pass through the cell membrane cause some negative changes in both the structure and functions of some important biomolecules (such as DNA, Proteins). As a result of these interactions, they activate Caspase enzymes, which play a role in cell death mechanisms such as apoptosis, with the increase of ROS. In addition, they affect mitochondrial permeability and increase cytochrome c release, increasing the propagation of signals to cause apoptosis and causing cell death (Rolim et al. 2019; Webster 2020; Barabadi et al. 2020; Donga et al. 2020; Hosny et al. 2022a).

Table 3- Percent viability rates as a result of cytotoxic effects of synthesized AuNPs on 48 h cell lines (*n*=3, $\bar{X} \pm S\bar{x}$, 48 Hours)

Cell Lines	***25*** *µg/mL*	***50*** *µg/mL*	***100*** *µg/mL*	***200*** *µg/mL*
HDF	86.74±0.011	80.07±0.012	56.52±0.013	14.64±0.030
U118	87.82±0.090	83.78±0.042	76.77±0.044	73.43±0.049
CaCo-2	69.24±0.008	43.17±0.003	33.27±0.003	12.25±0.019
Sk-ov-3	73.90±0.003	66.85±0.008	60.07±0.006	52.15±0.019

Cancer cells: **Caco-2**; Human Colorectal Adenocarcinoma, **U118**; Human Glioblastoma, and **Skov-3**; Human Healthy cells: **HDF;** Human Dermal Fibroblast

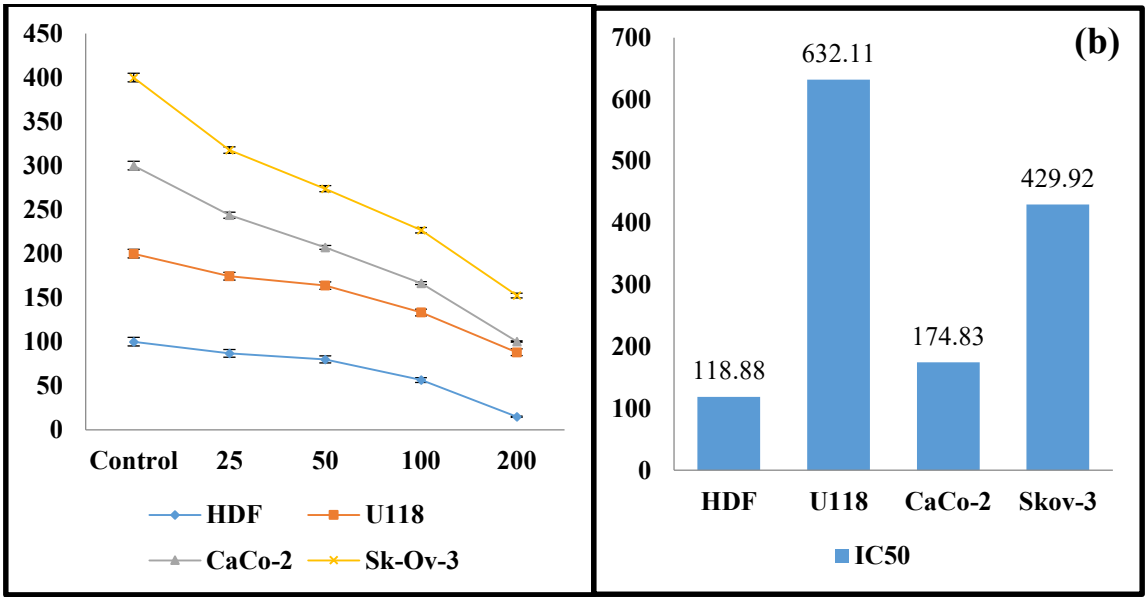

Figure 10- (a) Percent survival rates as a result of the interaction of the synthesized AuNPs with the cell lines for 48 hours via the MTT method, (b) IC50 values of the AuNPs on the cell lines

It was stated that AuNPs synthesized using *Cystoseira baccata* extract were effective on CaCo-2 cancer cells at a concentration of 400 µg/mL (González-Ballesteros et al. 2017). It has been reported that AuNPs synthesized with *Hygrophila spinosa* extract at a concentration of 47.5 µg/mL have a role in suppression of percent viability (Satpathy et al. 2020b). In addition, in some studies, it was reported that AuNPs obtained by green synthesis on different cancer cell lines showed anticancer effects with the MTT method (Chellamuthu et al. 2019; Chellapandian et al. 2019; Webster 2020).

4. Conclusions

N. sativa plant has many medicinal benefits. For this reason, the demand for its production continues to increase day by day. As a result of the products, a large part of the green parts of the plant remains as agricultural waste. In this study, AuNPs were rapidly synthesized with a low-cost, environmentally friendly approach by using the extract prepared from these parts of the plant to recycle these agricultural waste parts into a useful area. The characterization of AuNPs from *N. sativa* leaf extract was determined by UV-vis, XRD, EDX, Zeta potential and Zetasizer, FESEM, AFM, and TGA-DTA. It was observed that the morphology of AuNPs with a maximum absorbance of 538.41 nm was spherical, with a size distribution of 107 nm and monodisperse. The AuNPs synthesized with a surface charge of -17.7 mV were stable. For the usability of AuNPs as biomedical agents, antimicrobial and anticancer effects were investigated using microdilution and the MTT methods, respectively. AuNPs were effective on hospital pathogens at very low concentrations in the range of 0.02-1.00 µg/mL concentrations. The percent viability on cancer cell lines especially CaCo-2 significantly suppressed on cancer cells.

The significant suppression that AuNPs synthesised with the waste parts of N. sativa extract show on the pathogenic strains and cancer cells used in practise demonstrates that they have the potential to make a significant contribution to the search for anticancer and antimicrobial agents by improving the conditions under which they are synthesised. It is possible that the evaluation of this in-vitro study in vivo will be of major value to the medical field. It is also possible to undertake a large number of research to investigate its impact on various cancer cells and pathogenic strains.

References

Abu-Dief A M, Abdel-Rahman L H, Abd-El Sayed M A, Zikry M M & Nafady A (2020). Green Synthesis of AgNPs Ultilizing Delonix Regia Extract as Anticancer and Antimicrobial Agents. *Chemistry Select* 5(42): 13263–13268. https: //doi.org/10.1002/slct.202003218

Ahmad T, Bustam M A, Irfan M, Moniruzzaman M, Anwaar Asghar H M, & Bhattacharjee S (2018). Green synthesis of stabilized spherical shaped gold nanoparticles using novel aqueous Elaeis guineensis (oil palm) leaves extract. *Journal of Molecular Structure* 1159: 167–173. https://doi.org/10.1016/j.molstruc.2017.11.095

Ahmed K B A, Raman T & Veerappan A (2016). Future prospects of antibacterial metal nanoparticles as enzyme inhibitor. *Materials Science and Engineering C* 68: 939–947. https://doi.org/10.1016/j.msec.2016.06.034

Ahmed M J, Murtaza G, Rashid F & Iqbal J (2019). Eco-friendly green synthesis of silver nanoparticles and their potential applications as antioxidant and anticancer agents. *Drug Development and Industrial Pharmacy I 45:*1682–1694. https://doi.org/10.1080/03639045.2019.1656224

Aktepe N, Baran A, Atalar M N, Baran M F, Düz M Z, Yavuz Ö, İrtegün Kandemir S & Kavak D E (2021). Biosynthesis of Black Mulberry Leaf Extract and Silver NanoParticles (AgNPs): Characterization, Antimicrobial and Cytotoxic Activity Applications. *MAS Journal of Applied Sciences* 8(8): 685–700. https://doi.org/10.52520/masjaps.120

Al-ogaidi I, Salman M I, Mohammad F I, Aguilar Z, Al, M, Hadi Y A, & Al-rhman R M A (2017). Antibacterial and Cytotoxicity of Silver Nanoparticles Synthesized in Green and Black Tea. *World Journal of Experimental Biosciences* 5(1): 39–45. https://wjebio.com/index.php/journal/article/view/118

Ariamanesh H, Tamizi N, Yazdinezhad A, Salah S, Motamed N & Amanloo S (2019). The Effectiveness of *Nigella Sativa* Alcoholic Extract on the Inhibition of *Candida Albicans* Colonization and Formation of Plaque on Acrylic Denture Plates: an In Vitro Study. *Journal of Dentistry* 20(3): 171–177. https://doi.org/10.30476/dentjods.2019.44911

Arroyo G V, Madrid A T, Gavilanes A F, Naranjo B, Debut A, Arias M T & Angulo Y (2020). Green synthesis of silver nanoparticles for application in cosmetics. *Journal of Environmental Science and Health - Part A Toxic/Hazardous Substances and Environmental Engineering* 55(11): 1304–1320. https://doi.org/10.1080/10934529.2020.1790953

Atalar M N, Baran A, Baran M F, Keskin C, Aktepe N, Yavuz Ö & İrtegun Kandemir S (2021). Economic fast synthesis of *olive leaf* extract and silver nanoparticles and biomedical applications. *Particulate Science and Technology* 2021: 1–9 https://doi.org/10.1080/02726351.2021.1977443

Attar A & Yapaoz M A (2018). Biosynthesis of palladium nanoparticles using Diospyros kaki leaf extract and determination of antibacterial efficacy. *Preparative Biochemistry and Biotechnology* 48(7): 629–634. https://doi.org/10.1080/10826068.2018.1479862

Awad M A, Eisa N, Virk P, Hendi A A, Ortashi K, Mahgoub A A, Elobeid M M & Eissa F (2019). Green synthesis of gold nanoparticles: Preparation, characterization, cytotoxicity, and anti-bacterial activities. *Materials Letters* 256: 126608. https://doi.org/10.1016/j.matlet.2019.126608

Babu B, Palanisamy S, Vinosha M, Anjali R, Kumar P, Pandi B, Tabarsa M, You S G & Prabhu N M (2020). Bioengineered gold nanoparticles from marine seaweed Acanthophora spicifera for pharmaceutical uses: antioxidant, antibacterial, and anticancer activities. *Bioprocess and Biosystems Engineering* 43(12): 2231–2242. https://doi.org/10.1007/s00449-020-02408-3

Barabadi H, Webster T, Vahidi H, Sabori H, Damavandi Kamali K, Jazayeri Shoushtari F, Mahjoub M A, Rashedi M, Mostafavi E, Medina Cruz D, Hosseini O & Saravana M (2020). Green nanotechnology-based gold nanomaterials for hepatic cancer therapeutics: A systematic review. *Iranian Journal of Pharmaceutical Research* 19(3): 3–17. https://doi.org/10.22037/ijpr.2020.113820.14504

Baran M F (2018). Green Synthesıs Of Sılver Nanopartıcles (AgNPs) Usıng *Pistacia terebinthus* Leaf: Antimicrobial Effect And Characterization. *EJONS International Journal on Mathematic, Engineering and Natural Sciences* 2: 67–75

Baran M F (2018). Green Synthesıs Of Sılver Nanopartıcles (AgNPs) Usıng *Pistacia terebinthus* Leaf: Antimicrobial Effect And Characterization. *EJONS International Journal on Mathematic, Engineering and Natural Sciences* 2: 67–75

Baran M F (2019). Evaluation of Green Synthesis and Anti-Microbial Activities of AgNPs Using Leaf Extract of Hawthorn Plant. *Research and Evaluations in Science and Mathematics* 2019(3): 110–120

Baran M F& Saydut A (2019). Gold nanomaterial synthesis and characterization. *Dicle University Journal of Engineering* 10(3): 1033–1040. https://doi.org/10.24012/dumf.551865

Baran M F, Keskin C, Atalar M N & Baran A (2021). Environmentally Friendly Rapid Synthesis of Gold Nanoparticles from Artemisia absinthium Plant Extract and Application of Antimicrobial Activities. *Journal of the Institute of Science and Technology* 11(1): 365–375. https://doi.org/10.21597/jist.779169

Baran A, Baran M F, Keskin C, Kandemir S I, Valiyeva M, Mehraliyeva S, Khalilov R & Eftekhari A (2021a). Ecofriendly/Rapid Synthesis of Silver Nanoparticles Using Extract of Waste Parts of Artichoke (*Cynara scolymus L.*) and Evaluation of their Cytotoxic and Antibacterial Activities. *Journal of Nanomaterials* 2021: 1–10. https://doi.org/10.1155/2021/2270472

Baran A, Keskin C, Baran M F, Huseynova I, Khalilov R, Eftekhari A, Irtegun-Kandemir S & Kavak D E (2021b). Ecofriendly Synthesis of Silver Nanoparticles Using Ananas comosus Fruit Peels: Anticancer and Antimicrobial Activities. *Bioinorganic Chemistry and Applications* 2021: 058149, https://doi.org/10.1155/2021/2058149

Chellamuthu C, Balakrishnan R, Patel P, Shanmuganathan R, Pugazhendhi A & Ponnuchamy K (2019). Gold nanoparticles using red seaweed Gracilaria verrucosa: Green synthesis, characterization and biocompatibility studies. *Process Biochemistry 80(2):58-63* 0–1. https://doi.org/10.1016/j.procbio.2019.02.009

Chellapandian C, Ramkumar B, Puja P, Shanmuganathan R, Pugazhendhi A & Kumar P (2019). Gold nanoparticles using red seaweed Gracilaria verrucosa: Green synthesis, characterization and biocompatibility studies. *Process Biochemistry* 8010: 58–63. https://doi.org/10.1016/j.procbio.2019.02.009

Chen J, Li Y, Fang G, Cao Z, Shang Y, Alfarraj S, Ali Alharbi S, Duan X, Yang S & Li J (2021). Green synthesis, characterization, cytotoxicity, antioxidant, and anti-human ovarian cancer activities of *Curcumae kwangsiensis* leaf aqueous extract green-synthesized gold nanoparticles. *Arabian Journal of Chemistry* 14(3): 103000. https://doi.org/10.1016/j.arabjc.2021.103000

Chen X, Xue Z, Ji J, Wang D, Shi G, Zhao L & Feng S (2021). Hedysarum polysaccharides mediated green synthesis of gold nanoparticles and study of its characteristic, analytical merit, catalytic activity. *Materials Research Bulletin* 133(7): 111070. https://doi.org/10.1016/j.materresbull.2020.111070

Cui Y, Zhao Y, Tian Y, Zhang W, Lü X & Jiang X (2012). The molecular mechanism of action of bactericidal gold nanoparticles on Escherichia coli. *Biomaterials* 33(7): 2327–2333. https://doi.org/10.1016/j.biomaterials.2011.11.057

Dadigala R, Guttena V, Kotu G M, Bandi R, Gangapuram B R & Alle M (2018). Microwave assisted rapid green synthesis of gold nanoparticles using Annona squamosa L peel extract for the efficient catalytic reduction of organic pollutants. *Journal of Molecular Structure* 1167: 305–315. https://doi.org/10.1016/j.molstruc.2018.05.004

Davoudi-Kiakalayeh A, Mohammadi R, Pourfathollah A A, Siery Z & Davoudi-Kiakalayeh S (2017). Alloimmunization in thalassemia patients: New insight for healthcare. *International Journal of Preventive Medicine* 8(101): 1–7. https://doi.org/10.4103/ijpvm.IJPVM

Doan V D, Thieu A T, Nguyen T D, Nguyen V C, Cao X T, Nguyen T L H & Le V T (2020). Biosynthesis of Gold Nanoparticles Using Litsea cubeba Fruit Extract for Catalytic Reduction of 4-Nitrophenol. *Journal of Nanomaterials* 2020(1): 1–10. https://doi.org/10.1155/2020/4548790

Donga S, Bhadu G R & Chanda S (2020). Antimicrobial, antioxidant and anticancer activities of gold nanoparticles green synthesized using Mangifera indica seed aqueous extract. *Artificial Cells, Nanomedicine and Biotechnology* 48(1): 1315–1325. https://doi.org/10.1080/21691401.2020.1843470

Ercan L (2023). Investigation of Antibacterial and Antifungal Efficacy of Zinc and Silver Nanoparticles Synthesized from Nasturtium officinale. *Journal of Agricultural Sciences* 29(3): 788-799. https://doi.org/10.15832/ankutbd.1163132

Ferreyra Maillard A P V, Dalmasso P R, López de Mishima B A & Hollmann A (2018). Interaction of green silver nanoparticles with model membranes: possible role in the antibacterial activity. *Colloids and Surfaces B: Biointerfaces* 171(7): 320–326. https://doi.org/10.1016/j.colsurfb.2018.07.044

Firdhouse M J & Lalitha P (2020). Facile synthesis of anisotropic gold nanoparticles and its synergistic effect on breast cancer cell lines. *IET Nanobiotechnology* 14(3): 224–229. https://doi.org/10.1049/iet-nbt.2019.0279

Francis S, Joseph S, Koshy E P & Mathew B (2017). Green synthesis and characterization of gold and silver nanoparticles using Mussaenda glabrata leaf extract and their environmental applications to dye degradation. *Environmental Science and Pollution Research* 24: 17347–17357. https://doi.org/10.1007/s11356-017-9329-2

Giljohann D A, Seferos D S, Daniel W L, Massich M D, Patel P C & Mirkin C A (2010). Gold nanoparticles for biology and medicine. *Angewandte Chemie - International Edition* 49(19): 3280–3294. https://doi.org/10.1002/anie.200904359

González-Ballesteros N, Prado-López S, Rodríguez-González J B, Lastra M & Rodríguez-Argüelles M C (2017). Green synthesis of gold nanoparticles using brown algae Cystoseira baccata: Its activity in colon cancer cells. *Colloids and Surfaces B: Biointerfaces* 153: 190–198. https://doi.org/10.1016/j.colsurfb.2017.02.020

Gopinath K, Kumaraguru S, Bhakyaraj K, Mohan S, Venkatesh K S, Esakkirajan M, Kaleeswarran P, Alharbi N S, Kadaikunnan, S, Govindarajan M, Benelli G & Arumugam A (2016). Green synthesis of silver, gold and silver/gold bimetallic nanoparticles using the Gloriosa superba leaf extract and their antibacterial and antibiofilm activities. *Microbial Pathogenesis* 101:1 1–11. https://doi.org/10.1016/j.micpath.2016.10.011

Hatipoğlu A (2021a). Green synthesis of gold nanoparticles from Prunus cerasifera pissardii nigra leaf and their antimicrobial activities on some food pathogens. *Progress in Nutrition* 23(3): e2021241. https://doi.org/10.23751/pn.v23i3.11947

Hatipoğlu A (2021b). Rapid green synthesis of gold nanoparticles : synthesis , characterization , and antimicrobial activities. *Progress in Nutrition* 23(3): e2021242. https://doi.org/10.23751/pn.v23i3.11988

Hosny M, Fawzy M, Abdelfatah A M, Fawzy E E & Eltaweil A S (2021). Comparative study on the potentialities of two halophytic species in the green synthesis of gold nanoparticles and their anticancer, antioxidant and catalytic efficiencies. *Advanced Powder Technology* 32(9): 3220–3233. https://doi.org/10.1016/j.apt.2021.07.008

Hosny, M., Fawzy, M., El-Badry, Y. A., Hussein, E. E., & Eltaweil, A. S. (2022b). Plant-assisted synthesis of gold nanoparticles for photocatalytic, anticancer, and antioxidant applications. *Journal of Saudi Chemical Society* 26(2): 101419. https://doi.org/10.1016/j.jscs.2022.101419

Hosny M, Fawzy M, El-Borady O M & Mahmoud A E D (2021). Comparative study between Phragmites australis root and rhizome extracts for mediating gold nanoparticles synthesis and their medical and environmental applications. *Advanced Powder Technology* 32(7): 2268–2279. https://doi.org/10.1016/j.apt.2021.05.004

İş Ş & Beyatlı A (2023). Biological and Pharmacological Properties of Black Cumin (Nigella sativa). *Mersin University Faculty of Medicine Lokman Hekim Journal of Medical History and Folkloric Medicine* 13(3): 543–552. https://doi.org/10.31020/mutftd.1310960 (In Turkish)

Jafarizad A, Safaee K, Vahid B, Khataee A & Ekinci D (2019). Synthesis and characterization of gold nanoparticles using Hypericum perforatum and Nettle aqueous extracts: A comparison with turkevich method. *Environmental Progress and Sustainable Energy* 38(2): 508–517. https://doi.org/10.1002/ep.12964

Jha P, Saraf A, Rath D & Sharma D (2017). Green Synthesis and Antimicrobial Property of Gold Nanoparticles : a Review. *World Journal of Pharmaceutıcal and Medıcal Research* 3(8): 431–435.

Khan A U, Khan M, Malik N, Cho M H & Khan M M (2019). Recent progress of algae and blue–green algae-assisted synthesis of gold nanoparticles for various applications. *Bioprocess and Biosystems Engineering* 42(1): 1–15. https://doi.org/10.1007/s00449-018-2012-2

Korani S, Rashidi K, Hamelian M, Jalalvand A R, Tajehmiri A, Korani M, Sathyapalan T & Sahebkar A (2021). Evaluation of Antimicrobial and Wound Healing Effects of Gold Nanoparticles Containing Abelmoschus esculentus (L.) Aqueous Extract. *Bioinorganic Chemistry and Applications* 2021(1): 1–13. https://doi.org/10.1155/2021/7019130

Kumar V, Singh D K, Mohan S, Gundampati R K & Hasan S H (2017). Photoinduced green synthesis of silver nanoparticles using aqueous extract of Physalis angulata and its antibacterial and antioxidant activity. *Journal of Environmental Chemical Engineering* 5(1): 744–756. https://doi.org/10.1016/j.jece.2016.12.055

Kumar V, Singh S, Srivastava B & Bhadouria R (2019). Journal of Environmental Chemical Engineering Green synthesis of silver nanoparticles using leaf extract of Holoptelea integrifolia and preliminary investigation of its antioxidant , anti- in fl ammatory , antidiabetic and antibacterial activities. *Journal of Environmental Chemical Engineering* 7(3): 103094. https://doi.org/10.1016/j.jece.2019.103094

Kumari A, Naveen Dhatwalia J, Thakur S, Radhakrishnan A, Chauhan A, Chandan G, Choi B H & Neetika N (2023). Antioxidant, antimicrobial, and cytotoxic potential of Euphorbia royleana extract-mediated silver and copper oxide nanoparticles. *Chemical Papers* 77(8): 4643–4657. https://doi.org/10.1007/s11696-023-02814-3

Küp F Ö, Çoşkunçay S & Duman F. (2020). Biosynthesis of silver nanoparticles using leaf extract of Aesculus hippocastanum (horse chestnut): Evaluation of their antibacterial, antioxidant and drug release system activities. *Materials Science and Engineering C* 107: 110207. https://doi.org/10.1016/j.msec.2019.110207

Latha D, Prabu P, Gnanamoorthy G, Munusamy S, Sampurnam S, Arulvasu C & Narayanan V (2019). Size-dependent catalytic property of gold nanoparticle mediated by Justicia adhatoda leaf extract. *SN Applied Sciences* 1(134): 1–14. https://doi.org/10.1007/s42452-018-0148-y

Mandhata C P, Sahoo C R, Mahanta C S & Padhy R N (2021). Isolation, biosynthesis and antimicrobial activity of gold nanoparticles produced with extracts of Anabaena spiroides. *Bioprocess and Biosystems Engineering* 44(8): 1617–1626. https://doi.org/10.1007/s00449-021-02544-4

Mehravani B, Ribeiro A I & Zille A. (2021). Gold nanoparticles synthesis and antimicrobial effect on fibrous materials. *Nanomaterials* 11(5): 1–37. https://doi.org/10.3390/nano11051067

Mohammadi F, Yousefi M & Ghahremanzadeh R (2019). Green Synthesis , Characterization and Antimicrobial Activity of Silver Nanoparticles (AgNps) Using Leaves and Stems Extract of Some Plants. *Advanced Journal of Chemistry-Section A* 2(4): 266–275. https://doi.org/10.33945/SAMI/AJCA.2019.4.1

Mousavi-Kouhi S M, Beyk-Khormizi A, Mohammadzadeh V, Ashna M, Es-haghi A, Mashreghi M, Hashemzadeh V, Mozafarri H, Nadaf M & Taghavizadeh Yazdi M E (2022). Biological synthesis and characterization of gold nanoparticles using Verbascum speciosum Schrad. and cytotoxicity properties toward HepG2 cancer cell line. *Research on Chemical Intermediates* 48(1): 167–178. https://doi.org/10.1007/s11164-021-04600-w

Mythili R, Selvankumar T, Srinivasan P, Sengottaiyan A, Sabastinraj J, Ameen F, Al-sabri A, Kamala-kannan S, Govarthanan M & Kim H (2018). Biogenic synthesis , characterization and antibacterial activity of gold nanoparticles synthesised from vegetable waste. *Journal of Molecular Liquids* 262(7): 318–321. https://doi.org/10.1016/j.molliq.2018.04.087

Nor Azlan A Y H, Katas H, Jalluddin N Q & Fauzi Mh Busra M (2020). Gold nanoparticles biosynthesized using Lignosus rhinocerotis extracts: comparative evaluation of biostatic and cytotoxicity Effects. *Sains Malaysiana* 49(7): 1697–1712. https://doi.org/10.17576/jsm-2020-4907-20

Padalia H & Chanda S (2021). Antioxidant and Anticancer Activities of Gold Nanoparticles Synthesized Using Aqueous Leaf Extract of *Ziziphus nummularia*. *BioNanoScience* 11(2): 281–294. https://doi.org/10.1007/s12668-021-00849-y

Parida U K, Bindhani B K & Nayak P (2011). Green Synthesis and Characterization of Gold Nanoparticles Using Onion (*Allium cepa*) Extract. *World Journal of Nano Science and Engineering* 01(04): 93–98. https://doi.org/10.4236/wjnse.2011.14015

Parveen R, Ullah S, Sgarbi R & Tremiliosi-Filho G (2019). One-pot ligand-free synthesis of gold nanoparticles: The role of glycerol as reducing-cum-stabilizing agent. *Colloids and Surfaces A: Physicochemical and Engineering Aspects* 565(10): 162–171. https://doi.org/10.1016/j.colsurfa.2019.01.005

Patil M P, Singh R D, Koli P B, Patil, K T, Jagdale B S., Tipare A R & Kim G (2018). Antibacterial potential of silver nanoparticles synthesized using *Madhuca longifolia* flower extract as a green resource. *Microbial Pathogenesis* 121(8): 184–189. https://doi.org/10.1016/j.micpath.2018.05.040

Patra S, Mukherjee S, Kumar A, Ganguly A, Sreedhar B & Ranjan C (2015). Green synthesis , characterization of gold and silver nanoparticles and their potential application for cancer therapeutics. *Materials Science & Engineering C* 53(8): 298–309. https://doi.org/10.1016/j.msec.2015.04.048

Perveen K, Husain F M, Qais F A, Khan A, Razak S, Afsar T, Alam P, Almajwal A M & Abulmeaty M M A (2021). Microwave-assisted rapid green synthesis of gold nanoparticles using seed extract of trachyspermum ammi: Ros mediated biofilm inhibition and anticancer activity. *Biomolecules* 11(2): 1–16. https://doi.org/10.3390/biom11020197

Punnoose M S & Mathew B (2022). Microwave-assisted green synthesis of Cyanthillium cinereum mediated gold nanoparticles: Evaluation of its antibacterial, anticancer and catalytic degradation efficacy. *Research on Chemical Intermediates* 48(3): 1025–1044. https://doi.org/10.1007/s11164-021-04641-1

Rauf A, Ahmad T, Khan A, Maryam Uddin G, Ahmad B, Mabkhot Y N, Bawazeer S, Riaz N, Malikovna B K, Almarhoon Z. M & Al-Harrasi A (2021). Green synthesis and biomedicinal applications of silver and gold nanoparticles functionalized with methanolic extract of *Mentha longifolia*. *Artificial Cells, Nanomedicine and Biotechnology* 49(1): 194–203. https://doi.org/10.1080/21691401.2021.1890099

Rautray S & Rajananthini A U (2020). Therapeutic potential of green, synthesized gold nanoparticles. *BioPharm International*, *33*(1): 30–38.

Remya R R, Rajasree S R R, Aranganathan L & Suman T Y (2015). An investigation on cytotoxic effect of bioactive AgNPs synthesized using Cassia fistula flower extract on breast cancer cell MCF-7. *Biotechnology Reports* 22(8): 110–115. https://doi.org/10.1016/j.btre.2015.10.004

Rolim W R, Pelegrino M T, de Araújo Lima B, Ferraz L S, Costa F N, Bernardes J S, Rodigues T, Brocchi M & Seabra A B (2019). Green tea extract mediated biogenic synthesis of silver nanoparticles: Characterization, cytotoxicity evaluation and antibacterial activity. *Applied Surface Science* 463(1): 66–74. https://doi.org/10.1016/j.apsusc.2018.08.203

Satpathy S, Patra A, Ahirwar B & Hussain M D (2020a). Process optimization for green synthesis of gold nanoparticles mediated by extract of *Hygrophila spinosa T*. Anders and their biological applications. *Physica E: Low-Dimensional Systems and Nanostructures* 121(3): 113830. https://doi.org/10.1016/j.physe.2019.113830

Seku K, Gangapuram B R, Pejjai B, Hussain M, Hussaini S S, Golla N & Kadimpati K K (2019). Eco-friendly synthesis of gold nanoparticles using carboxymethylated gum *Cochlospermum gossypium* (CMGK) and their catalytic and antibacterial applications. *Chemical Papers* 73(7): 1695–1704. https://doi.org/10.1007/s11696-019-00722-z

Sepahvand M, Buazar F & Sayahi M H (2020). Novel marine-based gold nanocatalyst in solvent-free synthesis of polyhydroquinoline derivatives: Green and sustainable protocol. *Applied Organometallic Chemistry* 34(12): 1–11. https://doi.org/10.1002/aoc.6000

Shankar P D, Shobana S, Karuppusamy I, Pugazhendhi A, Ramkumar V S, Arvindnarayan S & Kumar G (2016). A review on the biosynthesis of metallic nanoparticles (gold and silver) using bio-components of microalgae: Formation mechanism and applications. *Enzyme and Microbial Technology* 95(1): 28–44. https://doi.org/10.1016/j.enzmictec.2016.10.015

Singh A K, Tiwari R, Singh V K, Singh P, Khadim S R, Singh U, Laxmi Srivastava V, Hasan S H & Asthana R K (2019). Green synthesis of gold nanoparticles from Dunaliella salina, its characterization and in vitro anticancer activity on breast cancer cell line. *Journal of Drug Delivery Science and Technology* 51(6): 164–176. https://doi.org/10.1016/j.jddst.2019.02.023

Some S, Bulut O, Biswas K, Kumar A, Roy A, Sen I K, Mandal A, Franco O L, İnce İ A, Neog K, Das S, Pradhan S, Dutta S, Bhattacharjya D, Saha S, Das Mohapatra P. K, Bhuimali A, Unni B G Kati A & Ocsoy I (2019). Effect of feed supplementation with biosynthesized silver nanoparticles using leaf extract of Morus indica L. V1 on Bombyx mori L. (Lepidoptera: Bombycidae). *Scientific Reports* 9(1): 1–13. https://doi.org/10.1038/s41598-019-50906-6

Suriyakala G, Sathiyaraj S, Babujanarthanam R, Alarjani K M, Hussein D S, Rasheed R A & Kanimozhi K (2022). Green synthesis of gold nanoparticles using Jatropha integerrima Jacq. flower extract and their antibacterial activity. *Journal of King Saud University - Science* 34(3): 101830. https://doi.org/10.1016/j.jksus.2022.101830

Swamy M K, Akhtar M S, Mohanty S K & Sinniah U R (2015). Synthesis and characterization of silver nanoparticles using fruit extract of *Momordica cymbalaria* and assessment of their *in vitro* antimicrobial, antioxidant and cytotoxicity activities. *Spectrochimica Acta - Part A: Molecular and Biomolecular Spectroscopy* 151(12): 939–944. https://doi.org/10.1016/j.saa.2015.07.009

Ullah N, Odda A H, Li D, Wang Q & Wei Q (2019). One-pot green synthesis of gold nanoparticles and its supportive role in surface activation of non-woven fibers as heterogeneous catalyst. *Colloids and Surfaces A: Physicochemical and Engineering Aspects* 571(January): 101–109. https://doi.org/https://doi.org/10.1016/j.colsurfa.2019.03.076

Umamaheswari C, Lakshmanan A & Nagarajan N S (2018). Green synthesis, characterization and catalytic degradation studies of gold nanoparticles against congo red and methyl orange. *Journal of Photochemistry and Photobiology B: Biology* 178(8): 33–39. https://doi.org/10.1016/j.jphotobiol.2017.10.017

Usman A I, Aziz A A & Noqta O A (2019). Green sonochemical synthesis of gold nanoparticles using palm oil leaves extracts. *Materials Today: Proceedings* 7(3): 803–807. https://doi.org/10.1016/j.matpr.2018.12.078

Uzma M, Prasad D, Sunayana N, Vinay R & Shilpashree H (2021). Studies of *in vitro* antioxidant and anti-inflammatory activities of gold nanoparticles biosynthesised from a medicinal plant, *Commiphora wightii*. *Materials Technology* 37(9): 915–925. https://doi.org/10.1080/10667857.2021.1905206

Velmurugan P, Anbalagan K, Manosathyadevan M, Lee K J, Cho MinJung-Hee Park Sae-Gang Oh K S B, Oh B-T & Lee S M. (2014). Green synthesis of silver and gold nanoparticles using Zingiber officinale root extract and antibacterial activity of silver nanoparticles against food pathogens. *Bioprocess and Biosystems Engineering* 37(10): 1935–1943. https://doi.org/10.1007/s00449-014-1169-6

Vinita Nirala N R & Prakash R (2018). One step synthesis of AuNPs@MoS2-QDs composite as a robust peroxidase- mimetic for instant unaided eye detection of glucose in serum, saliva and tear. *Sensors and Actuators, B: Chemical* 263(6): 109–119. https://doi.org/10.1016/j.snb.2018.02.085

Webster T J (2020). Recent Developments in the Facile Bio-Synthesis of Gold Nanoparticles (AuNPs) and Their Biomedical Applications. *International Journal of Nanomedicine* 2020(15): 275–300. https://doi: 10.2147/IJN.S233789

Zayadi R A, Abu Bakar F & Ahmad M K (2019). Elucidation of synergistic effect of eucalyptus globulus honey and *Zingiber officinale* in the synthesis of colloidal biogenic gold nanoparticles with antioxidant and catalytic properties. *Sustainable Chemistry and Pharmacy* 13(March): 100156. https://doi.org/10.1016/j.scp.2019.100156